Hindawi Publishing Corporation
Physical Separation in Science and Engineering
Volume 2007, Article ID 34832, 7 pages
doi:10.1155/2007/34832

Research Article

Liquid-Liquid Interfacial Transport of Nanoparticles

Stefanie Machunsky and Urs Alexander Peuker

Received 23 March 2007; Revised 29 August 2007; Accepted 8 November 2007

Recommended by Hermann Nirschl

The study presents the transfer of nanoparticles from the aqueous phase to the second nonmiscible nonaqueous liquid phase. The transfer is based on the sedimentation of the dispersed particles through a liquid-liquid interface. First, the colloidal aqueous dispersion is destabilised to flocculate the particles. The agglomeration is reversible and the flocs are large enough to sediment in a centrifugal field. The aqueous dispersion is laminated above the receiving organic liquid phase. When the particles start to penetrate into the liquid-liquid interface, the particle surface is covered with the stabilising surfactant. The sorption of the surfactant onto the surface of the primary particles leads to the disintegration of the flocs. This phase transfer process allows for a very low surfactant concentration within the receiving organic liquid, which is important for further application, that is, synthesis for polymer-nanocomposite materials. Furthermore, the phase transfer of the nanoparticles shows a high efficiency up to 100% yield. The particle size within the organosol corresponds to the primary particle size of the nanoparticles.

1. INTRODUCTION

Typical strategies for the wet nanoparticle synthesis are precipitation, reduction, or comminution processes. Mostly, these processes are conducted in aqueous phase. A growing number of applications of nanoparticle dispersions, for example, self-organised coating of surfaces and composite materials [1, 2], require a nonaqueous liquid phase. Therefore, after synthesis the nanoparticles have to be transferred from the aqueous liquid to a nonaqueous liquid for further use.

Conventional strategies for this phase transfer, which are known from micron-scale particles, are based on filtration, drying, and redispersion steps. This strategy cannot be applied, because the quality and functionality [3] of nanoparticles strongly suffer when submitted to a gas phase; irreversible agglomeration, oxidation, and sintering occur. Thus, for these small particle sizes below 100 nm, a different strategy is necessary, which is the direct liquid-liquid phase transfer.

In this field, fundamental work is done in lab scale. With the help of surfactants, which adsorb at the particle surface, the wetting of hydrophilic particles by organic liquids becomes possible. The application of a surfactant supports the transfer through the liquid-liquid interface and further has stabilising effects to prevent agglomeration within the organic phase.

Most systematic research on the phase transfer of nanoparticles is conducted on gold and silver hydrosols [4–9], which are synthesised via a reduction reaction at a low concentration (10^{-3} to 10^{-5} g/L). Directly after synthesis, the hydrosol is stabilised either with an adsorbed hydrophilic surfactant or electrostatically with the help of an increased surface charge. For phase transfer, the receiving liquid phase contains a second surfactant [8, 10, 11]. In the millilitre scale, the mass transport of the particles to the liquid-liquid interface is promoted by vigorous stirring or shaking. During this mixing, the surfactant can react with the water droplets dispersed in the organic phase and the two liquids are emulsified [9]. This undesired effect requires further processing to separate and break the emulsion again.

The need of nanoparticles in organic liquids requires the process development of technical and scaleable transfer processes. One promising approach is the direct phase transfer of sedimenting particles through a defined liquid-liquid interface.

2. THEORETICAL BACKGROUND

2.1. Description of the transfer process

The phase transfer by sedimentation through a liquid-liquid interface uses the gravitational or the centrifugal force to create a relative movement of the particles within the suspension liquid. The second liquid, which receives the particles, has a higher specific weight than the releasing liquid. The receiving and releasing liquids have to be nonmiscible. The

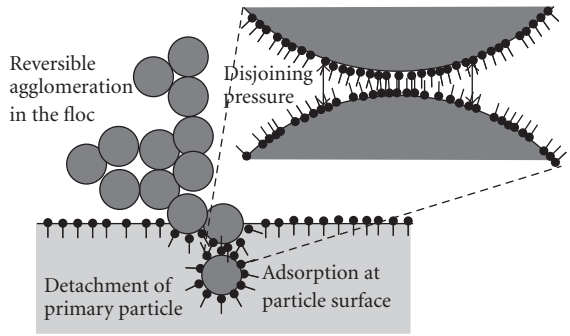

Figure 1: Mechanism of phase transfer and deagglomeration in the presence of surfactant molecules at the interface.

aqueous suspension (releasing liquid) is laminated above the receiving organic liquid. Subsequently, the sedimentation in the gravitational or centrifugal field is started (see Figure 5). To increase the sedimentation speed of the nanoparticles in the releasing aqueous phase, the dispersion is destabilised by reducing the electrostatic particle-particle interaction. This is done by adjusting the pH to change the surface charge and the zeta potential, respectively. This change in electrostatic repulsion should be done carefully such that the particles are trapped in the second minimum of the DLVO-potential curve. Even when the particle-liquid interactions do not show a secondary minimum in the potential curve and the electrostatic stabilisation in the aqueous phase is not possible, the strong repulsive potential of adsorbed surfactant molecules is able to overcome the agglomeration in the organic phase. The deagglomeration is a function of the geometry, the surface coverage, the adsorption equilibrium, and the solubility of the surfactant in the organic phase.

The choice of the surfactant is the key point for the phase transfer and deagglomeration step at the liquid-liquid interface. The surfactant has to adsorb at the particle surface. This adsorption changes the surface properties from hydrophilic to hydrophobic. Due to this desired hydrophobicity, the applied surfactants are mainly nonsoluble or poorly soluble in the releasing water phase (see Table 2). The surfactant is dosed into the organic phase. The adsorption isotherm of the surfactant on the particle surface determines the required concentration in the receiving organic liquid.

The phase transfer begins when the sedimenting floc arrives at the liquid-liquid interface. The surfactant concentration is enriched at the interface. The hydrophilic end of the surfactant reaches into the aqueous phase. This end adsorbs at the surface of the primary particle which is still incorporated in the floc. It is supposed that the adsorption occurs at the entire particle surface including that area, which is in closest distance to the neighbouring primary particle (see Figure 1). The adsorption of the surfactant molecules in this narrow gap creates an additional repulsing force, the disjoining pressure. When a certain surface coverage with surfactant molecules is reached, the disjoining pressure has the possibility to liberate the primary particles from the floc.

The adsorption of the surfactant disintegrates the flocculated nanoparticle system. Due to the stabilising effect of the surfactant, the particle size within the organic phase corresponds to the primary particle size (see Figure 4). The sedimentation velocity in the organic phase is considerably slower, which is due to the smaller size of the dispersed particles. In the gravitational field, the nanoparticles (magnetite) remain in suspension.

2.2. Particle-particle interactions

The efficiency of the transfer process and the deagglomeration are determined by the sorption of the surfactant on the particle surface. The surfactant cover changes the wetting and acts stabilising on the organic colloid. It further induces the deagglomeration in the organic phase.

The repulsive particle-particle interactions derive from the steric/osmotic interaction of the adsorbed surfactant molecules. In this paper, the magnetite particles and oleic acid (C18-carboxylic acid) are used. Even though oleic acid is a quite short molecule, its unperturbed radius of gyration R_G, which is the size of the coiled molecule within the solvent, can be calculated as

$$R_G = \frac{l \cdot \sqrt{M/M_0}}{\sqrt{6}}. \tag{1}$$

In this calculation, it is assumed that all distances between the single segments (CH_2-group) of the molecule are equal even though oleic acid possesses a double bond and a carboxyl group. The unperturbed radius of gyration of oleic acid then amounts to $R_G = 0.275$ nm.

At low concentration, a monolayer of adsorbed coiled molecules covers the surface. As a rough guide [12], the maximum coverage without overlap occurs when all molecules coils lie flat and in dense packing on the surface. The minimum distance s between two molecules hence is twice the unperturbed radius of gyration:

$$s_{\min} = 2 \cdot R_G. \tag{2}$$

The coverage per unit area Γ can be calculated from the distance between the adsorbed molecules:

$$\Gamma = \frac{1}{s^2}. \tag{3}$$

At the maximum monolayer coverage, the distance s is equal to $s_{\min}$. Thus, for oleic acid, the maximum monolayer coverage $\Gamma_{\max}$ is 3.3 molecules per square nanometer. At a higher coverage, the structure of the adsorbed layer changes. The coils are squeezed, and molecules with one coupling end and a longer tail (like oleic acid) align parallel to each other. This structure is called brush.

The consumption of surfactant can be calculated from the coverage per unit area. The results for a spherical 10 nm magnetite particle, which has a surface of 314 nm^2 (S_v = 0.6 nm^2/nm^3), are shown in Table 1.

This rough calculation of the coverage fits to measurements of oleic acid adsorption on precipitated magnetite (0.5–2 μm) using the solvent CCl_4 [13]. The adsorption isotherm shows the typical shape. The transition point from the monolayer Langmuir regime to the multilayer regime

Table 1: Monolayer adsorption of oleic acid onto magnetite particles (10 nm).

Coverage Γ of the particle surface (nm^{-2})	Molecules adsorbed per particle (−)	Mass ratio surfactant per solid matter (g_{surf}/g_{solid})
$\Gamma_{max} = 3.3$	1037	0.178
$0.5*\Gamma_{max} = 1.7$	518	0.089
$0.1*\Gamma_{max} = 0.3$	104	0.018

is located at about 1 vol.% oleic acid concentration within the solvent. The surface coverage at that point amounts to about 25 molecules per square nanometer. This is eight times higher than the maximal packing of coiled molecules (Γ_{max}). Thus, monolayer adsorption does not end until the surfactant has reached brush configuration on the surface. In this brush configuration, each stretched molecule oleic acid covers an anchoring area of 0.2 × 0.2 nanometers. These measurements [13] further show that the adsorbed number of molecules in multilayer adsorption strongly increases above 2.5–3 vol.% oleic acid concentration.

The repulsive interaction energy per unit area [14] between two surfactant covered flat surfaces is given in the interval $2R_G < D < 8R_G$ by the approximation

$$W = 36 \cdot \Gamma \cdot k \cdot T \cdot e^{-(D/R_G)}, \tag{4}$$

which assumes that coiled molecules ($\Gamma < \Gamma_{max}$) are involved in the interaction. This repulsive interaction competes for the stabilisation as well as the deagglomeration with the attractive v.d. Waals interaction

$$W = -\frac{A}{12 \cdot \pi \cdot D^2}. \tag{5}$$

The plot of the ratio of steric to v.d. Waals interaction (see Figure 2) shows the intense repulsion of the surfactant layers. The higher the coverage Γ of the surface is, the higher the repulsion becomes. At surface coverage Γ_{max}, the steric repulsion is more than one order of magnitude, higher than the attractive v.d. Waals potential. Even at $\Gamma = 0.1\ \Gamma_{max}$, the repulsive force is able to overcome the v.d. Waals attraction in the interval of 1–4 R_G.

The integral interaction potential (see (6)) of steric stabilisation is plotted for the magnetite oleic acid system in Figure 3. It shows the typical minimum that derives from the short-range repulsive steric/osmotic potential, which dominates near the surface. Compared to the osmotic potential, the v.d. Waals potential has a long-range action. The minimum in the potential curve shows that in the organic phase, the particles are not entirely separated from each other, but they are trapped in a distance of some R_G. It needs further energy input to liberate the single particles:

$$W_{\int} = W_{vdW} + W_{steric} = -\frac{A}{12 \cdot \pi \cdot D^2} + 36 \cdot \Gamma \cdot k \cdot T \cdot e^{-(D/R_G)}. \tag{6}$$

In the deagglomeration process, which occurs during the sorption of the surfactant oleic acid, the distance between the particles grows. The adsorbed surfactant molecules, even at low coverage of the particle surface, create high repulsive potential, which is able to overcome the v.d. Waals potential. During the deagglomeration process, the characteristic length and the gap between the particles (see Figure 1), respectively, run from below R_G to some R_G, and the potential follows the curves plotted in Figure 3. The distance between the particles grows until the interaction potential has become zero.

When the mass transport and the adsorption kinetics are slower than the process of deagglomeration, the deagglomeration already starts before the surface coverage has reached its equilibrium. Thus, during the disjoining process, the surface coverage still increases. This further coverage of the surface

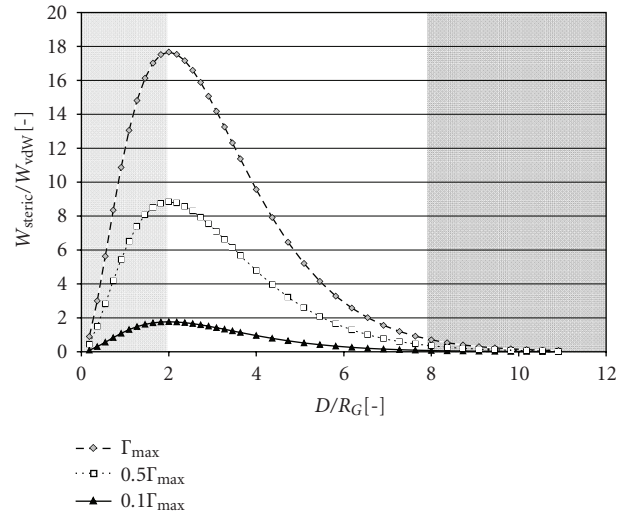

Figure 2: Ratio of repulsive steric to attractive v.d. Waals interaction between two flat oleic acid covered magnetite surfaces in dichloromethane ($A = 4.3\ 10^{-20}$ J, $T = 300$ K); white: area of validity of (4).

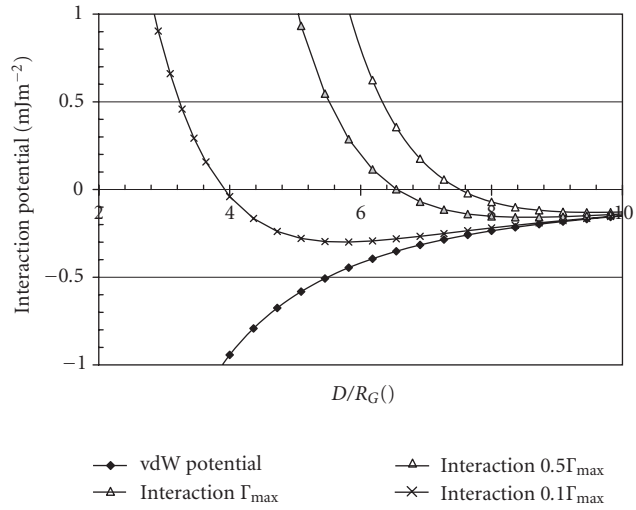

Figure 3: Integral interaction potential (see (6)) of steric stabilisation of an oleic acid covered flat magnetite surface in dichloromethane for different surface coverage Γ.

shifts the minimum along with the rest position of the two particles to higher distances.

For future calculation of the absolute value of the repulsive potential and the rest position, the geometric orientation of the particles, as well as their geometry itself, has to be considered.

3. MATERIAL AND METHODS

3.1. Chemicals

Oleic acid, iron(II)sulfate heptahydrate ($Fe_3O_4 * 7H_2O$) and iron(III)chloride hexahydrate ($FeCl_3 * 6H_2O$), dichloromethane (DCM), and ammonium hydroxide (26% NH_3) are purchased from Fluka AG (Switzerland) and used as received.

3.2. Precipitation of magnetite particles

The magnetite nanoparticles are produced by coprecipitation of an aqueous solution of iron(III)chloride hexahydrate and iron(II)sulfate heptahydrate with a molar ratio of $Fe^{3+}/Fe^{2+} = 2 : 1$. The iron solution is precipitated with concentrated ammonium hydroxide in excess. The precipitation process is done with vigorous stirring in a glass beaker. The iron salts are dissolved in distilled water and heated to 70°C. The amount of ammonium hydroxide is quickly added to the resulting solution, producing deep black magnetite precipitates at once. The suspension has been stirred for another 30 minutes at 70°C in order to evaporate any trace ammonium salts. Due to the high pH of 9-10 and zeta potential of −10 mV, the flocculation of the nanomagnetite already occurs in this step.

3.3. Particle characterisation

Particle size in diluted liquid phase has been measured with photon correlation spectroscopy (PCS, Malvern Instruments Zetasizer Nano ZS). In organic phase, the surfactant concentration is kept constant during dilution. The magnetite concentration in the aqueous phase after precipitation, and in the organic phase after phase transfer, is quantified with a spectrophotometer at 590 nm (DR 4000, Hach Company, Colo, USA) applying the 1.10 phenanthroline method. The water content within the samples has been measured using Karl Fischer titration.

3.4. Experimental setup for phase transfer

Two different setups have been used for the experiments. Setup 1 is a simple measuring beaker in which the sedimentation occurs (see Figure 5(a)). In the gravity field, the sedimentation time amounted to 24 hours. All liquids are cooled down to ambient temperature. The magnetite was synthesised at the same day directly prior to the phase transfer experiments.

First, the organic liquid with a higher specific weight than water is filled into the beaker. The organic liquid is dichloromethane, which contains oleic acid as surfactant. The initial volume concentration of oleic acid amounts to 1–10 vol.%. Then, the aqueous magnetite suspension is laminated above organic phase. The flocculation has already occurred during the precipitation step (see Figure 4).

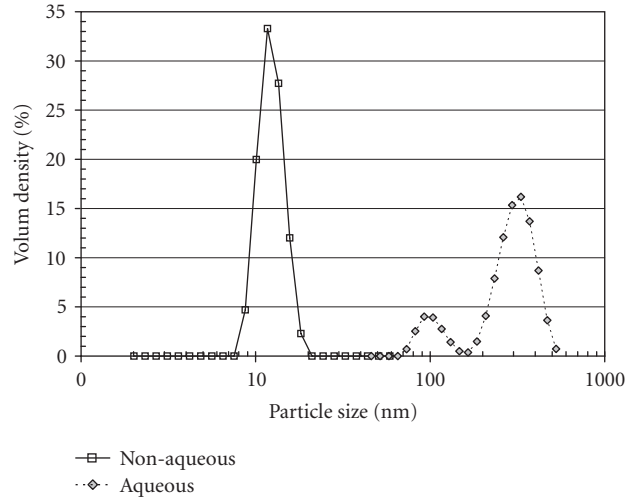

Figure 4: Particle size of precipitated magnetite (Fe_3O_4) at pH 7 in releasing aqueous and receiving dichloromethane phases, and surfactant mass ratio of 0.4 $g_{oleic\ acid}/g_{magnetite}$.

Table 2: Properties of the organic phase.

	Density (kg/L)	Solubility in water (20°C) (g/L)	HLB	Hansen solubility parameter δ_t
Dichloromethane (CCl_2H_2)	1.33	20	—	20.3
Oleic acid ($C_{18}H_{34}O_2$)	0.89	—	1 [15]	15.6

The Hettich Universal 16 lab-scale centrifuge (143 mm effective radius, 100 mL centrifuge glasses) has been used as experimental setup 2 (see Figure 5(b)). The preparation of the samples in the centrifuge glasses is identical to that in the beaker experiments: filling of organic liquid and laminating the (flocculated) aqueous suspension above. The samples then are centrifugated for 60 minutes at 4000 1/min (2558 g).

After the sedimentation either in the centrifugal or the gravity field, the aqueous phase is removed and samples are taken from both the organic liquid and the aqueous liquid to determine solids content and the particle size. In the organic phase, additionally the water content is quantified.

4. EXPERIMENTAL RESULTS

The main aim is the development of a liquid-liquid phase transfer process which leads to a minimal content of the surfactant within the received organosol. Therefore, the transfer process along with the surfactant dosage has to be optimised. The surfactant content in the organosol is directly coupled to its concentration in the receiving phase. The quality of the organosol for further processing depends on the ratio of surfactant to solid. The smaller this ratio is, the smaller the quantity of nonadsorbed free surfactant will be. This free

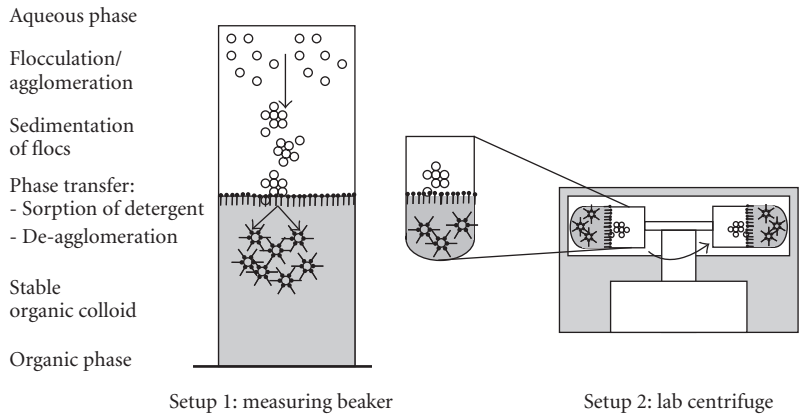

Figure 5: (a) Experimental setup 1 used for sedimentation in the gravitational field; (b) experimental setup 2, lab-scale beaker centrifuge with maximum centrifugal number $C = 4000$.

surfactant has a negative influence on the quality, for example, that of the incorporation of magnetite into composite materials made on the basis of the organosol [16, 17].

The experiments have been carried out in the gravitational and centrifugal fields (not shown). Magnetite tends to agglomerate in the aqueous phase. Due to its low surface charge (−5 mV at pH 7), electrostatic stabilisation of the dispersion after precipitation is not possible. The poor stability of the precipitated particles is already an advantage for the transfer process of the nanoparticles. After the precipitation and the removal of ammonium chloride, the suspension is already flocculated (see Figure 4) and no additional conditioning or change of pH, respectively, is necessary. The magnetite agglomerates sediment towards the interface even in the gravitational field when the water-based magnetite dispersion is laminated above the receiving organic phase (dichloromethane).

The experiments have been conducted with two mass ratios of surfactant (oleic acid) to solid. The mass ratio of surfactant to solid is controlled by the volume ratio of the releasing to the receiving phase (see (7)). The higher mass ratio of surfactant to solid has been adjusted by using more receiving liquids with the constant surfactant concentration:

$$\frac{m_{\text{surf}}}{m_{\text{solid}}} = \frac{\rho_{\text{surf}} \cdot V_{\text{surf}}}{m_{\text{solid}}} = \frac{\rho_{\text{surf}} \cdot (c_{\text{surf}}/(1 - c_{\text{surf}}))V_{\text{receiving}}}{m_{\text{solid}}}. \tag{7}$$

The lower ratio is 0.448 $g_{\text{oleic acid}}/g_{\text{magnetite}}$ and the higher ratio is 0.895 $g_{\text{oleic acid}}/g_{\text{magnetite}}$. This corresponds to a maximum coverage (all oleic acid molecules adsorbed) of 8.3 at the lower concentration and 16.6 at the higher concentration, respectively; molecules oleic acid per square nanometer on the surface of a 10 nm particle. This is more than twice the number of molecules needed for a dense monolayer packing on the 10 nm particle. It can be stated that the dosage of oleic acid is sufficient to ensure a full coverage of the magnetite in the organic phase, which is necessary to change the wetting properties and to create the strong steric repulsion for deagglomeration.

The experimental results are plotted: yield of the transfer as a function of the surfactant concentration in the receiving phase. The yield is defined as a fraction of the particles being transferred to the organic phase. The 100% yield leads to a clear and transparent releasing liquid. The ratio of surfactant to solid particles is kept constant for each experimental series.

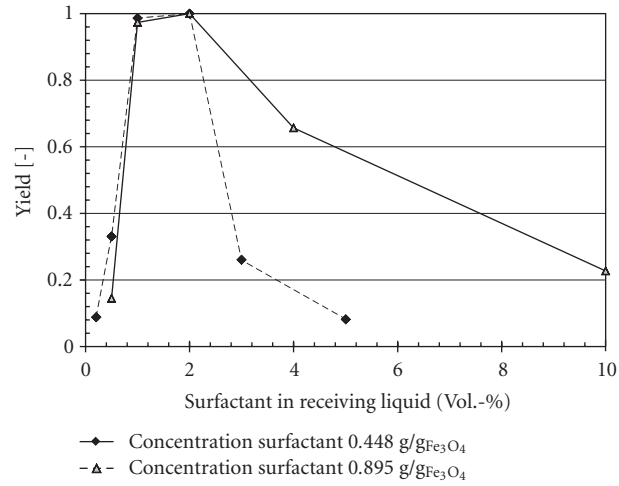

Figure 6: Phase transfer of magnetite nanoparticles subsequent to precipitation (24-hour gravity settling).

At low concentration of surfactant (<1 vol.%), only a partial transfer occurs (see Figure 6). The yield is below 50%. The low concentration influences the adsorption equilibrium at the particle surface. Even though enough surfactant molecules are present in the receiving phase at the low concentration, these molecules do not attach in a sufficient number to the particle surface to change the wetting properties to hydrophobic. The nontransferred particles build up a sediment on the liquid-liquid interface.

With increasing the initial surfactant concentration to 1-2 vol.%, the yield reaches 100%. All particles are transported through the interface into the organic liquid. The agglomerates pass the interface and the primary particles are liberated from the aggregates. The particle size within the organosol shows (after dilution) the primary size of the precipitated

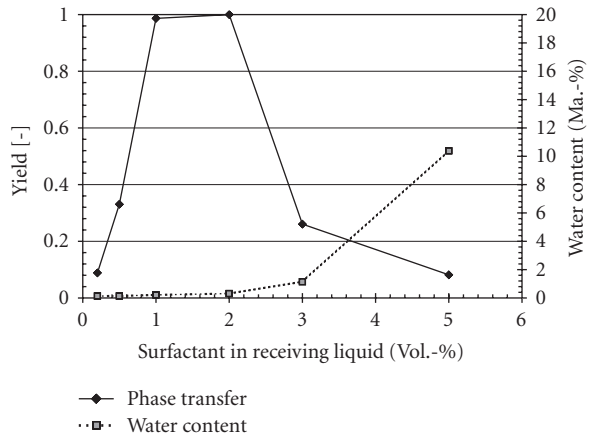

FIGURE 7: Trapped water during phase transfer of magnetite, and mass ratio of 0.448 $g_{oleic\ acid}/g_{magnetite}$ (24-hour gravity settling).

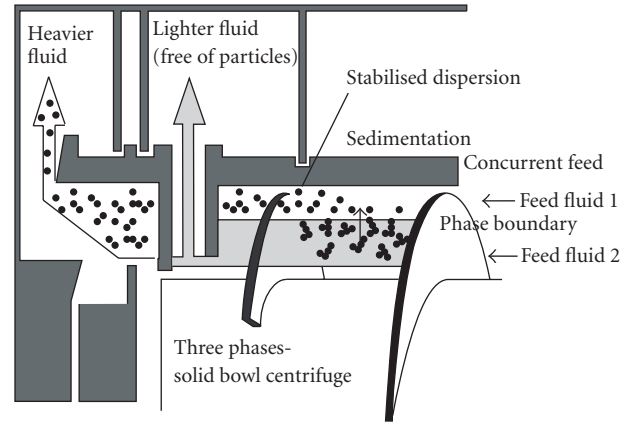

FIGURE 8: Phase transfer in technical scale using a concurrent decanting centrifuge.

magnetite (see Figure 4). Up to 2 vol.% surfactant concentration, the experimental curves for 0.448 $g_{oleic\ acid}/g_{magnetite}$ and 0.895 $g_{oleic\ acid}/g_{magnetite}$ are close to each other. In this concentration range, the mass ratio of surfactant to solid has no effect on the transfer process.

Further reduction of the mass ratio of oleic acid to solid is possible. The influence of the mass ratio on the transfer yield becomes detectable when it falls below 0.2 $g_{oleic\ acid}/g_{magnetite}$ (not shown). This mass ratio corresponds to a theoretic surface coverage of 3.6 molecules per square nanometer on a 10 nm particle, which is close to the calculated maximum coverage of coiled oleic acid, $\Gamma_{max} = 3.3$.

With further increase of the initial surfactant concentration above 2 vol.%, the yield decreases. The surfactant concentration of 2-3 vol.% corresponds to the transition point in the adsorption isotherm, where multilayer adsorption of the surfactant occurs [13]. The decrease is stronger at the lower mass ratio of surfactant to solid. At 5 vol.% surfactant concentration and mass ratio of 0.448 $g_{oleic\ acid}/g_{magnetite}$, the yield is about 10% even though the same quantity of surfactant molecules is available in the receiving phase.

With the decrease in the transfer yield, the water content in the receiving phase increases (see Figure 7). The maximum water content has been measured for a surfactant mass ratio of 0.4-0.5 $g_{oleic\ acid}/g_{magnetite}$. It amounts up to 10 mass%.

One explanation is that the solubility of water in dichloromethane increases with increasing surfactant concentration and the surfactant traps water within micelles, respectively. The water is transported with the agglomerate through the interface. This process is favoured by the high concentration of oleic acid within the receiving phase as well as the strong tendency of oleic acid to form micelles. The concentration of oleic acid for all experiments is above the critical micelle concentration (CMC) [13].

The surfactant molecules, which form water-filled micelles, are occupied and cannot adsorb at the magnetite surface. Hence, the effective mass ratio of surfactant to solid decreases and the surface coverage, which is coupled to the adsorption equilibrium, decreases as well. Finally, the surface coverage falls below that point, which allows for the transfer from hydrophilic to hydrophobic, and the transfer process is inhibited.

5. SCALE-UP

The centrifugation or sedimentation process has been chosen because of its scale-up perspective. Most lab-scale approaches use intense mixing (by shaking or stirring) and setting process, which has its own limitations in scale-up as well as in continuous operation and appropriate process equipment.

On the other hand, continuous centrifuges for sedimentation and phase separation are available with high centrifugal acceleration. Decanting centrifuges can be operated up to 4000–6000 g and disk stack centrifuges even up to 20.000 g. The three-phase decanter, which is used for the processing of liquid-liquid mixtures during centrifugal extraction, has a skimming tube to remove the heavier liquid (see Figure 8) and an overflow to retrieve the lighter phase.

The decanting centrifuge, when it is employed for the liquid-liquid phase transfer process, can be operated in concurrent mode; both feed fluxes are injected at the same side of the machine. With this conception, the particles have a maximum setting and a residence time within the centrifuge.

6. CONCLUSIONS

The sedimentation of flocculated magnetite nanoparticles through a liquid-liquid interface from the aqueous to the nonaqueous phase shows an optimum in the dosage of the surfactant oleic acid. The optimum concentration of surfactant in the receiving liquid dichloromethane amounts to 1-2 vol.%. Below this concentration, the surfactant does not adsorb with sufficiently high coverage onto the particle surface to hydrophobise it. Above this concentration, the organic phase (dichloromethane) incorporates water, which reduces the effect of the surfactant.

The adsorption of the surfactant allows for the transfer of the magnetite into the organic phase, and it further deagglomerates and stabilises the nanoparticles. Therefore, in the organic phase, the primary particle size is measured.

SYMBOLS

A: Hamaker const. (J)
c: Concentration (m^3/m^3)
D: Distance between interacting surfaces (m)
k: Boltzmann const. ($J\ K^{-1}$)
M: Mass of segment in molecule ($g\ mol^{-1}$)
m: Mass (kg)
M_0: Molar mass ($g\ mol^{-1}$)
R_G: Radius of gyration (m)
s: Distance (m)
T: Temperature (K)
V: Volume (m^3)
Γ: Coverage (m^{-2})
ρ: Density Indices ($kg\ m^{-3}$)
Surf: Surfactant
Solid: Solid particles

ACKNOWLEDGMENT

This project is funded by the German Research Foundation, Project no. PE1160/6-1.

REFERENCES

[1] T. Banert and U. A. Peuker, "Synthesis of magnetic beads for bio-separation using the solution method," *Chemical Engineering Communications*, vol. 194, no. 6, pp. 707–719, 2007.
[2] L. P. Ramírez and K. Landfester, "Magnetic polystyrene nanoparticles with a high magnetite content obtained by miniemulsion processes," *Macromolecular Chemistry and Physics*, vol. 204, no. 1, pp. 22–31, 2003.
[3] F. Caruso, "Nanoengineering of particle surfaces," *Advanced Materials*, vol. 13, no. 1, pp. 11–22, 2001.
[4] D. I. Gittins and F. Caruso, "Spontaneous phase transfer of nanoparticulate metals from organic to aqueous media," *Angewandte Chemie International Edition*, vol. 40, no. 16, pp. 3001–3004, 2001.
[5] A. Kumar, P. Mukherjee, A. Guha, et al., "Amphoterization of colloidal gold particles by capping with valine molecules and their phase transfer from water to toluene by electrostatic coordination with fatty amine molecules," *Langmuir*, vol. 16, no. 25, pp. 9775–9783, 2000.
[6] N. Lala, S. P. Lalbegi, S. D. Adyanthaya, and M. Sastry, "Phase transfer of aqueous gold colloidal particles capped with inclusion complexes of cyclodextrin and alkanethiol molecules into chloroform," *Langmuir*, vol. 17, no. 12, pp. 3766–3768, 2001.
[7] M. Sastry, A. Kumar, and P. Mukherjee, "Phase transfer of aqueous colloidal gold particles into organic solutions containing fatty amine molecules," *Colloids and Surfaces A*, vol. 181, no. 1–3, pp. 255–259, 2001.
[8] H. Yao, O. Momozawa, T. Hamatani, and K. Kimura, "Stepwise size-selective extraction of carboxylate-modified gold nanoparticles from an aqueous suspension into toluene with tetraoctylammonium cations," *Chemistry of Materials*, vol. 13, no. 12, pp. 4692–4697, 2001.
[9] S.-Y. Zhao, S.-H. Chen, D.-G. Li, and H.-Y. Ma, "Phase transfer of Ag nanoparticles by help of centrifugation," *Colloids and Surfaces A*, vol. 242, no. 1–3, pp. 145–149, 2004.
[10] W. Cheng and E. Wang, "Size-dependent phase transfer of gold nanoparticles from water into toluene by tetraoctylammonium cations: a wholly electrostatic interaction," *Journal of Physical Chemistry B*, vol. 108, no. 1, pp. 24–26, 2004.
[11] A. Swami, A. Kumar, and M. Sastry, "Formation of water-dispersible gold nanoparticles using a technique based on surface-bound interdigitated bilayers," *Langmuir*, vol. 19, no. 4, pp. 1168–1172, 2003.
[12] J. Israelachvili, *Intermolecular & Surface Forces*, Elsevier, San Diego, Calif, USA; Academic Press, London, UK, 2005.
[13] V. V. Korolev, A. G. Ramazanova, and A. V. Blinov, "Adsorption of surfactants on superfine magnetite," *Russian Chemical Bulletin*, vol. 51, no. 11, pp. 2044–2049, 2002.
[14] A. K. Dolan and S. F. Edwards, "Theory of the stabilization of colloids by adsorbed polymer," *Proceedings of the Royal Society of London A*, vol. 337, no. 1611, pp. 509–516, 1974.
[15] S. Yokoyama, J. Kouchi, T. Tabohashi, et al., "Emulsifying potency of new amino acid-type surfactant (II): stable water-in-oil (W/O) emulsions containing 85 wt% inner water phase," *Chemical & Pharmaceutical Bulletin*, vol. 49, no. 10, pp. 1331–1335, 2001.
[16] T. Banert and U. A. Peuker, "Production of highly filled Fe_3O_4/PMMA nanocomposites by the spraying process," *Chemie Ingenieur Technik*, vol. 77, no. 3, pp. 224–227, 2005.
[17] T. Banert and U. A. Peuker, "Preparation of highly filled superparamagnetic PMMA-magnetite nanocomposites using the solution method," *Journal of Materials Science*, vol. 41, no. 10, pp. 3051–3056, 2006.

AUTHOR CONTACT INFORMATION

Stefanie Machunsky: Institute of Chemical Engineering, Clausthal University of Technology, Leibnizstraße 17, 38678 Clausthal-Zellerfeld, Germany; machunsky@icvt.tu-clausthal.de

Urs Alexander Peuker: Institute of Chemical Engineering, Clausthal University of Technology, Leibnizstraße 17, 38678 Clausthal-Zellerfeld, Germany; urs.peuker@tu-clausthal.de